Imperfect Many-Body Localization in Exchange-Disordered Isotropic Spin Chains

To cite this article before publication: Julian Siegl *et al* 2023 *New J. Phys.* in press https://doi.org/10.1088/1367-2630/ad0e1b

Imperfect Many-Body Localization in Exchange-Disordered Isotropic Spin Chains

Julian Siegl* and John Schliemann
Institute for Theoretical Physics, University of Regensburg, Regensburg, Germany
(Dated: October 25, 2023)

We investigate many-body localization in isotropic Heisenberg spin chains with the local exchange parameters being subject to quenched disorder. Such systems incorporate a nonabelian symmetry in their Hamiltonian by invariance under global SU(2)-rotations. Nonabelian symmetries are predicted to hinder the emergence of a many-body localized phase even in the presence of strong disorder. We report on numerical studies using exact diagonalization for chains of common spin length 1/2 and 1. The averaged consecutive-gap ratios display a transition compatible with a crossover from an ergodic phase at small disorder strength to an incompletely localized phase at stronger disorder. Studying the sample-to-sample variance of the averaged consecutive-gap ratio, we distinguish this incompletely localized phase from the fully many-body localized phase by its scaling behavior.

I. INTRODUCTION

The equivalence of the classical notion of thermalization, i.e., that any appropriate subsystem of an isolated system is accurately described by equilibrium statistical mechanics, for isolated quantum systems is commonly taken to be the eigenstate thermalization hypothesis (ETH) [1–5]. Both fundamental questions regarding the transition from quantum to classical physics and its impact on measurable physical properties like conductivity [6–8] have motivated significant research into the validity of the ETH and how systems violate it [9]. A paradigmatic example of the latter is the Anderson insulator [6–8] where non-interacting electrons become localized in the presence of disorder and thus escape thermalization. After the early insights into the fate of localization for weak interaction and vanishing temperature [10–12], later works proved that interacting systems, typically in the presence of sufficiently strong disorder, also localize at finite temperature in a phenomenon dubbed *many-body localization* (MBL) [13–16]. Multiple toy models for numerical investigations were proposed, with one-dimensional disordered spin chains being commonly studied in the field, as they show signatures attributed to MBL [17–24]. While the issue of the critical disorder strength in such systems remains unsettled [25–34], there are arguments that most such models should enter a fully localized phase for sufficiently strong disorder [35]. This behavior is in contrast to systems displaying global nonabelian symmetries, where Potter and Vasseur [36] argued that the degeneracies imposed by their symmetry would inhibit the emergence of MBL even for arbitrarily strong disorder. Along these lines, Protopopov *et al.* [37, 38] performed numerical studies on disordered SU(2)-invariant spin chains using renormalization group approaches. They concluded the possibility of nonergodic phases different from the many-body localized one but found them to be unstable for increasing chain lengths. Related investigations on one dimensional Hubbard chains [39] also support the role of nonabelian symmetries in destabilizing the MBL phase [40–42]. Most recently, the effect of nonabelian symmetries on eigenstate thermalization [43] and entanglement entropies [44] has been discussed. In the present work, we report on a study of disordered rotationally invariant spin chains similar to Refs. [37, 38], but with different disorder distributions and with a focus on spectral properties. Specifically, we use the sample-to-sample variance of the expectation value of the consecutive-gap ratio [45] to distinguish the fate of this system at strong disorder. For the chain lengths accessible with this method, we identify a phase distinct both from the ergodic and the MBL phase in agreement with the phase proposed by Protopopov *et al.*. As the characteristics of this phase closely resemble the transient regime of the MBL transition, we refer to it as the *incompletely many-body localized phase*.

II. MODEL AND METHODS

We study isotropic Heisenberg spin chains with disordered local exchange parameters,

$$H_{\mathrm{ex}} = \sum_{i=1}^{N} J_i \vec{S}_i \cdot \vec{S}_{i+1}\,, \quad J_i = J + b_i\,, \tag{1}$$

* Julian.Siegl@ur.de

with $J \geq 0$, and $b_i \in [-b, b]$ being drawn from a uniform distribution [46] with disorder strength b. The characterization of this model as isotropic is due to the manifest invariance under global rotations of the spin direction as the Hamiltonian consists solely of a sum of inner products between spins. Each of these products is trivially invariant under a simultaneous rotation of all spins in the chain. The entire Hamiltonian thus adheres to a global symmetry identical to the free rotation of a single spin, as defined by the nonabelian symmetry group $SU(2)$. It is this global nonabelian symmetry of Eq. (1) that by the argument of Vasseur *et al.* should inhibit the emergence of MBL in this system. At sufficiently strong disorder $b \geq J$, some configurations of the disorder may realize a weak link $J_i \approx 0$ for at least one i with implications for the connectivity of the model's Hilbert space (see Appendix A for further discussion). Periodic boundary conditions are assumed, $\vec{S}_{i+N} = \vec{S}_i$, and we consider systems with common spin lengths $S = 1/2$ and $S = 1$. As the total spin $\vec{S}_{\text{tot}} = \sum_{i=1}^{N} \vec{S}_i$ commutes with the Hamiltonian, all energy levels lie in multiplets of $\vec{S}_{\text{tot}}$, which we account for in the following numerics. We perform exact diagonalization for fixed spin projections $S_{\text{tot,z}}$ and in the following considerations treat all multiplets except for those with quantum numbers $S_{\text{tot}} \in \{NS, NS-1\}$. Exploiting the fact that for each S_{tot} exactly one member of the multiplet lies in each subspace of fixed $S^z_{\text{tot}} \leq S_{\text{tot}}$, we start from the highest S^z_{tot} and successively eliminate further representatives of the same multiplet in lower S^z_{tot} subspaces. Thus, all gaps are calculated between levels of the same S_{tot} and S^z_{tot}.

Spectral properties of the Hamiltonian (Eq. (1)) are investigated via the consecutive-gap ratio r [25, 48] defined as

$$r_n = \frac{\min\{s_n, s_{n-1}\}}{\max\{s_n, s_{n-1}\}}, \tag{2}$$

where $s_n = e_{n+1} - e_n$ is the difference between neighboring energy levels e_{n+1}, e_n, each corresponding to a multiplet. The average $\langle r \rangle = \int_0^1 dr p(r) r$ of the random variable $r = r_n$ is determined by its probability distribution $p(r)$. Importantly, different phases reflect via the associated distributions in characteristic values for this averaged consecutive-gap ratio, making it a useful tool to elucidate phase transitions from the spectral information about a system. For integrable phases like the many-body localized phase, the level spacing follows Poissonian statistics [25], for which

$$p(r)|_{\text{Poisson}} = \frac{2}{(1+r)^2}. \tag{3}$$

The average consecutive gap ratio in this case is $\langle r \rangle = 2 \ln 2 - 1 \approx 0.3863$ [49], and the form of $p(r)$ for this case makes it apparent that consecutive levels do not repel in this case as the maximum value of the distribution is reached at $r = 0$. Contrary, random matrix theory predicts the ergodic phase with the symmetries of the Hamiltonian considered here [48] to follow the Gaussian orthogonal ensemble (GOE) for which

$$p(r)|_{\text{GOE}} = \frac{27}{4} \frac{r + r^2}{(1 + r + r^2)^{\frac{5}{2}}}. \tag{4}$$

Evaluating the average consecutive gap ratio with respect to the GOE prediction for $p(r)$ results in $\langle r \rangle = 4 - 2\sqrt{3} \approx 0.5359$. The level repulsion for the GOE ensemble is evident as $p(0) = 0$ in this case. By comparing the average consecutive gap ratio for the model in Eq. (1) under different disorder strengths to the known values for both the ergodic and the MBL phase, we can extract information about the phase transitions the model undergoes as the strength of disorder varies. The average $\langle r \rangle$ can be approximated by first calculating the average $\langle r \rangle_\alpha$ for a large number Q of disorder realizations (or samples) $\alpha \in \{1, \ldots, Q\}$ and then averaging the results,

$$\langle r \rangle = \lim_{Q \to \infty} \frac{1}{Q} \sum_{\alpha=1}^{Q} \langle r \rangle_\alpha \approx \frac{1}{Q} \sum_{\alpha=1}^{Q} \langle r \rangle_\alpha := \bar{r} \quad , \quad Q \gg 1 \,. \tag{5}$$

An additional measure for the presence of a phase transition can be constructed by exploiting the fact that the step-wise averaging in Eq. (5) contains additional statistical information, in addition to the average $\langle r \rangle$. Since the disorder realizations α are randomly chosen, the average consecutive gap ratio for a single realization α defines a random variable $x := \langle r \rangle_\alpha$, with probability distribution

$$s(x) = \frac{1}{(2b)^N} \int_{-b}^{b} db_1 \cdots \int_{-b}^{b} db_N \delta \left(x - \int_0^1 dr p(r; b_1, \ldots, b_N) r \right). \tag{6}$$

Here $p(r; b_1, \ldots, b_N) = p_\alpha$ is the probability distribution within a system with local modulations $b_1, \ldots, b_N$ on the exchange strength forming the disorder realization α. By construction, $s(x)$ has the property

$$\int_0^1 dx x s(x) = \int_0^1 dr r p(r) := \langle r \rangle_p = \langle r \rangle, \tag{7}$$

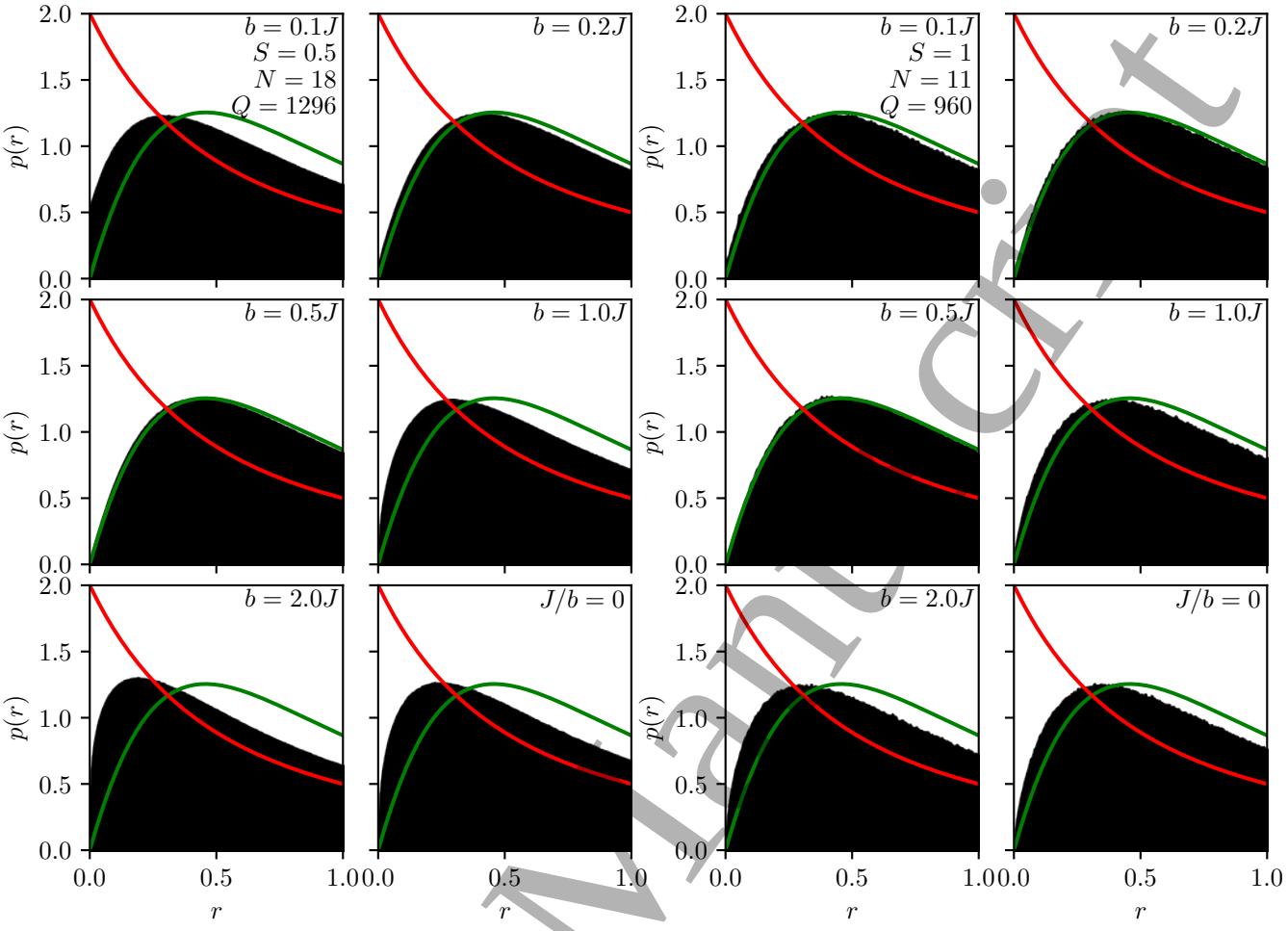

Figure 1. The probability distribution for the consecutive-gap ratio r of the multiplets of the isotropic spin chain (Eq. (1)) with spin lengths $S = 1/2$ (left) and $S = 1$ (right) for disorder b in terms of exchange interaction J ranging in strength from relatively weak $b = 0.1J$ to infinite disorder $J/b = 0$. The green and the red curves show the predictions for the ergodic (GOE) and the MBL phase (Poisson), respectively [48]. The distributions for both spin lengths first approach the GOE prediction as residual translational invariance is overcome. Around $b = J$, the distributions move away from GOE towards the MBL prediction. Both distributions remain distinct from the MBL case even at infinite disorder.

regardless of the fact that the distributions $p(r)$ and $s(x)$ do not generally coincide [45]. However, we can use $s(x)$ to interpret $\bar{r}$ in Eq. (5) as a sum over uncorrelated random variables with a joint distribution

$$\pi(x_1, \cdots, x_Q) = \prod_{\alpha=1}^{Q} s(x_\alpha)\,, \tag{8}$$

and an expectation value $\langle \bar{r} \rangle_\pi = \langle r \rangle_p$, where $\langle \cdot \rangle_{p/\pi}$ indicate the expectation value with respect to distribution $p(r)$ and $\pi(x_1, \cdots, x_Q)$ respectively. The sample-to-sample variance $(\Delta_s r)^2$ is defined as the variance of $s(x)$ is given by

$$(\Delta_s r)^2 = \int_0^1 dx (x - \langle r \rangle_p)^2 s(x). \tag{9}$$

The sample-to-sample variance is to be distinguished from the total variance $(\Delta_p r)^2$ with respect to the probability distribution $p(r)$. These two quantities are related via

$$(\Delta_p r)^2 = (\Delta_s r)^2 + \lim_{Q\to\infty} \frac{1}{Q} \sum_{\alpha=1}^{Q} (\Delta_\alpha r)^2\,, \tag{10}$$

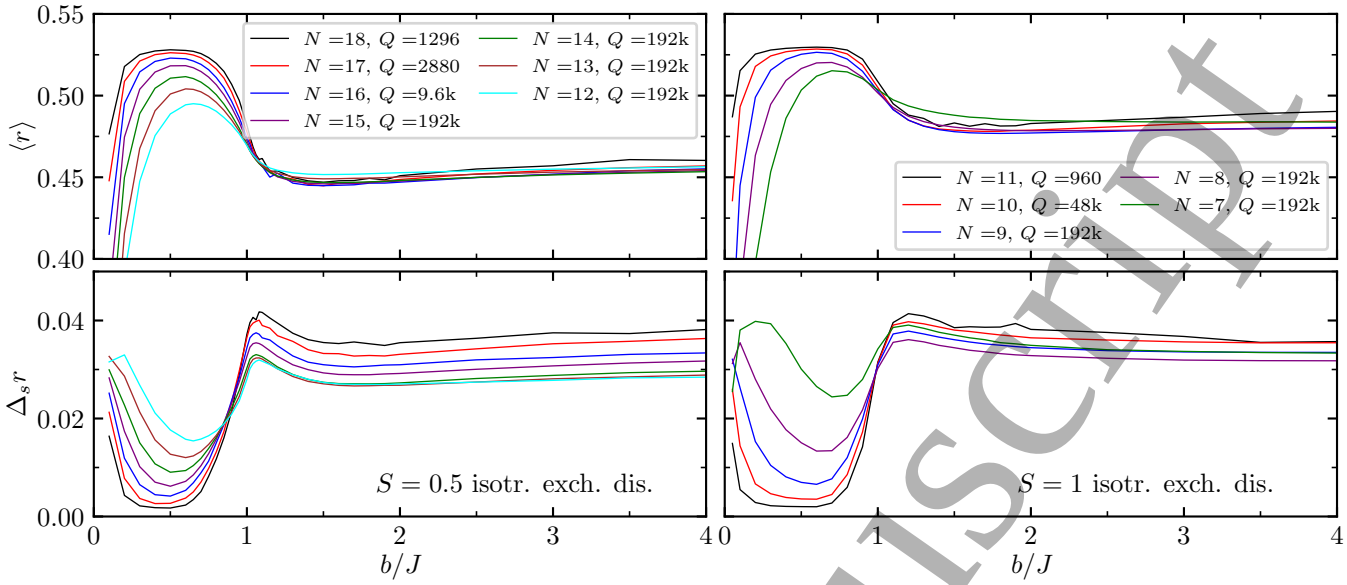

Figure 2. Top panels: The expectation value $\langle r\rangle$ as a function of disorder strength in chains of spin length $S = 1/2$ (left) and $S = 1$ (right) for spin chains of finite sizes N and pertaining numbers Q of disorder realizations. Bottom panels: The sample-to-sample standard deviation $\Delta_s r$ for the same parameters as in the top panels.

where $(\Delta_\alpha r)^2$ is the variance within the disorder realization α. The variance of $\bar{r}$ with respect to π reads

$$\langle(\bar{r} - \langle r\rangle_p)^2\rangle_\pi = \frac{1}{Q}(\Delta_s r)^2. \tag{11}$$

According to Eq. (11), a finite sample-to-sample variance indicates a convergence of $\bar{r}$ to $\langle r\rangle_p$ in mean square as Q^{-1}. Importantly, we can extract the sample-to-sample variance from our numerics via the approximate relation

$$(\Delta_s r)^2 \approx \frac{1}{Q}\sum_{\alpha=1}^{Q}(\langle r\rangle_\alpha - \bar{r})^2. \tag{12}$$

We are primarily interested in understanding the effect of the $SU(2)$ symmetry present in Eq. (1). Therefore, we will contrast our results with previous findings for a Heisenberg chain being subject to a disordered local field coupling to the z-component of each spin,

$$H_{\rm lf} = J\sum_{i=1}^{N}\vec{S}_i\cdot\vec{S}_{i+1} + 2S\sum_{i=1}^{N}h_i S_i^z\,, \tag{13}$$

with uniformly distributed local field strengths $h_i \in [-h, h]$. The disorder term in Eq. (13) is manifestly not invariant under global rotations of the spin direction, violating the $SU(2)$ symmetry of the exchange term in the same Hamiltonian. The local field disordered chain is commonly used in studies of many-body localization, particularly for spin length $S = 1/2$ [4, 9, 49–54]. Fewer works considered also larger spin lengths [45, 55, 56]. The local field disordered Heisenberg chain shows a transition from an ergodic phase at small disorder strength h to a many-body localized phase at large disorder. Numerical studies [20, 26, 27, 29, 57] have placed the critical disorder strength at values of $h_{\rm cr} \approx 4J$ or larger. Ref. [45] found, based on the sample-to-sample variance, a transition at $h_{\rm cr} \approx 2.6J \ldots 3.0J$ for $S = 1/2$, and $h_{\rm cr} \approx 4.0J \ldots 4.5J$ for $S = 1$. The nature and position of this transition have been critically discussed in recent publications in terms of matrix product states [32], Renyi entropies [58], quantum avalanches [59], Liouvillian relaxation [60], and time evolution [61].

III. RESULTS

Fig. 1 shows the disorder-averaged probability distribution $p(r)$ of the isotropic spin chain (Eq. (1)) in finite systems for spin lengths $S \in \{1/2, 1\}$. For small disorder, the system is in an ergodic phase, but the level repulsion predicted

from random matrix theory for the Gaussian orthogonal ensemble (GOE) is not perfectly recovered due to the approximate translational invariance present at weak disorder. This translational invariance results in degeneracies of the multiplets for vanishing disorder but gets lifted as soon as the local nature of the disorder becomes appreciable. At intermediate disorder $b =: b_{\mathrm{erg}} \approx 0.5J$ the data is practically indistinguishable from the GOE prediction given in Eq. (4). Importantly, with increasing disorder $p(r)$ does not remain aligned with the GOE prediction but shifts towards smaller values in a fashion similar to the transient regime observed before the onset of many-body localization in systems of the form of Eq. (13). Contrary to this transition, which has been thoroughly investigated in the literature, the distribution for the isotopically exchange-disordered spin chain does not reach, even for infinite disorder [62], the form expected for Poissonian statistics s given in Eq. (3). This is in line with the argument of Potter and Vasseur [36] which rules out the possibility of the emergence of a fully integrable phase due to the nonabelian symmetry incorporated in the Hamiltonian in Eq. (1).

In Fig. 2 we display the expectation value $\langle r\rangle$ along with the sample-to-sample standard deviation $\Delta_s r$ as a function of disorder strength b for spin chains of different lengths. Consistently with the findings from Fig. 1, the expectation value of the consecutive-gap ratio has a maximum at $b = b_{\mathrm{erg}} \approx 0.5J$, which moves with increasing system size close to the GOE value $\langle r\rangle \approx 0.5359$. At the same disorder strength, the sample-to-sample standard deviation reaches a minimum $(\Delta_s r)_{\mathrm{min}}$, and at larger $b =: b_{\mathrm{cr}} \gtrsim 1.0J$, a maximum $(\Delta_s r)_{\mathrm{max}}$ is attained while $\langle r\rangle$ shows an inflection point at about the same disorder strength.

The behavior of $(\Delta_s r)_{\mathrm{min}}$ and $(\Delta_s r)_{\mathrm{max}}$ as a function of system size N is shown in Fig. 3 (a). As seen there, $(\Delta_s r)_{\mathrm{min}}$ decreases monotonously, and the finite-size data is consistent with the assumption $(\Delta_s r)_{\mathrm{min}} \to 0$ for $N \to \infty$, while $(\Delta_s r)_{\mathrm{max}}$ increases with N. Thus, viewing the expectation value $\langle r\rangle$ as an order parameter, this quantity, along with the standard deviation $\Delta_s r$, shows as a function of disorder strength typical features of a phase transition. Analogous observations were made for the anisotropic chain (Eq. (13)) being subject to a local disordered field [45].

Let us now analyze the phase of the isotropic exchange-disordered spin chain (Eq. (1)) for disorder strengths larger than the critical value $b_{\mathrm{cr}} \gtrsim 1.0J$. As the top panels of Fig. 2 show, the average $\langle r\rangle$ of the consecutive-gap ratio lies here, for the system sizes N considered, between the value for Poissonian statistics and GOE statistics. However, $\langle r\rangle$ increases slightly with N, and a meaningful extrapolation turns out to be problematic; similar observations were made in Refs. [38, 63][64] Thus, just from the finite-size data for $\langle r\rangle$ at hand, it is difficult to argue that the system behaves in the thermodynamic limit $N \to \infty$ differently from a GOE ergodic phase.

A qualitative difference between the level statistics for $b > b_{\mathrm{cr}} \gtrsim 1.0J$ is, however, revealed by the sample-to-sample standard deviation $\Delta_s r$. Let us first discuss the case of spin length $S = 1/2$. As displayed in the top left panel of Fig. 3 (b), $\Delta_s r$ increases, at given disorder strength $b > b_{\mathrm{cr}}$, with system size (which is also seen in the bottom left panel of Fig. 2). This behavior is in contrast to the ergodic phase around $b = b_{\mathrm{erg}} \approx 0.5J$ where $\Delta_s r$ decreases with growing N (see also the top panels of Fig. 3 (a)), and the same is observed in the ergodic phase of the model (Eq. (13)) lacking a nonabelian symmetry [45]. Finally, in the bottom left panel of Fig. 3 (b) we have additionally plotted $\Delta_s r$ for the anisotropic Hamiltonian (Eq. (13)) at large disorder (where the system is many-body localized), and the sample-to-sample standard deviation also decreases with system size.

As of the case $S = 1$, $\Delta_s r$ as a function of N plotted in the top right panel of Fig. 3 (b) behaves differently from

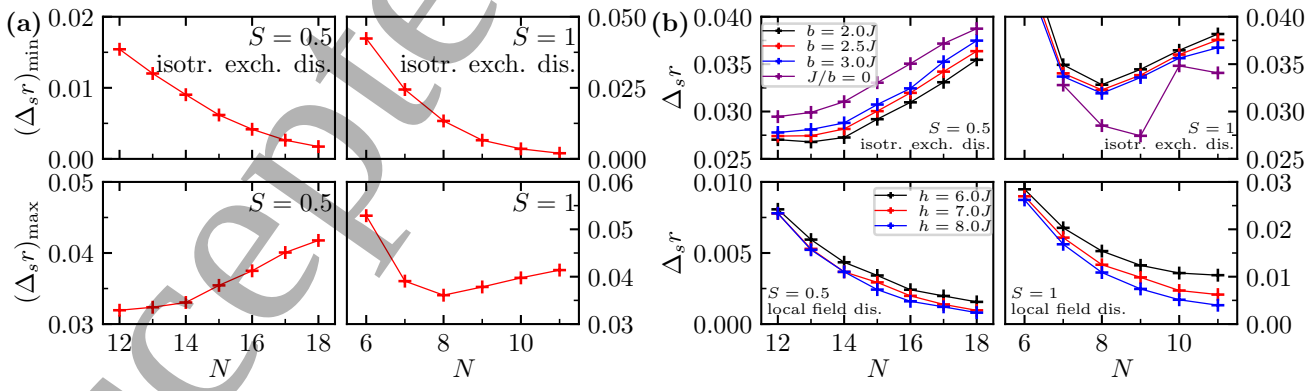

Figure 3. Scaling behavior of the sample-to-sample standard deviation's extremal values (a) and dependence on disorder strength (b) for different spin lengths as a function of system size N. The sample-to-sample standard deviation for spin length $S = 1/2$ (left) and $S = 1$ (right) shows a systematic decrease/increase for the minima (top panels in a) and maxima (bottom panels in a) respectively. The sample-to-sample standard deviation $\Delta_s r$ outside the ergodic phase for the isotropic disordered Heisenberg chain (Eq. (1)) (top panels in b) obeys different scaling from the equivalent regime in a chain (Eq. (13)) subject to a local disordered field (bottom panels in b). The data in the bottom panels is adopted from Ref. [45].

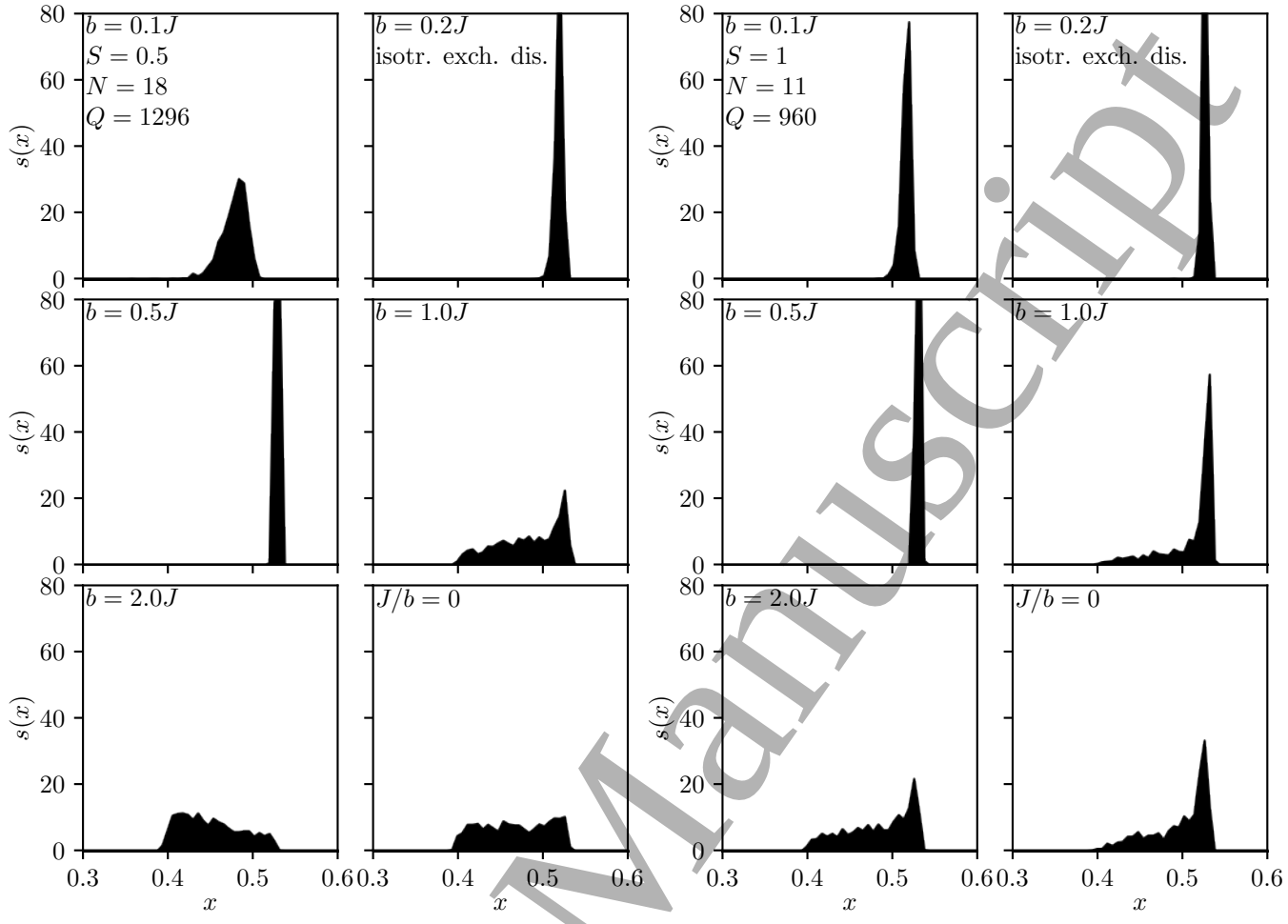

Figure 4. The probability distribution (Eq. (6)) for the realization-specific average $\langle r \rangle_\alpha$ for disordered Heisenberg chains of spin length $S = 1/2$ (left) and $S = 1$ (right). The disorder strengths b in both panels are the same as in Fig. 1.

the ergodic phase, but with less clear finite-size behavior. Moreover, this quantity decreases with growing disorder strength b, which is in contrast to $S = 1/2$ where the data smoothly increases with disorder strength.

In summary, the isotropic exchange-disordered spin chain (Eq. (1)) undergoes at a critical disorder strength $b_{\mathrm{cr}} \gtrsim 1.0J$ a transition from an ergodic phase to a phase that is neither ergodic nor fully many-body localized. As the nonergodic nature of this phase, even at strong disorder, is similar to the transient regime of the local field disordered chain (Eq. (13)) before integrability is reached, we refer to it as the *incompletely many-body localized phase*.

To verify that the system enters a phase distinct from both the ergodic and the MBL phase, we also investigated the probability distribution $s(x)$ for the realization-specific average $x := \langle r \rangle_\alpha$. at different disorder strengths. We plot it in Fig. 4 for the same representative values of the disorder strength as in Fig. 1. Starting from weak disorder, the distribution $s(x)$ narrows to a peak close to the GOE value $\langle r \rangle \approx 0.5359$ when approaching $b = b_{\mathrm{erg}} \approx 0.5J$. At the transition, $b =: b_{\mathrm{cr}} \gtrsim 1.0J$, $s(x)$ broadens, and remains of similar width for larger disorder. From the investigation of the local field disordered chain (Eq. (13)) conducted by Schliemann *et al.*, we can infer that under strong disorder conditions, the distribution should narrow to a peak around the value of $\langle r \rangle$ of 0.386 if the system were to become fully many-body localized [45]. Consequently, the shape of the probability distribution $s(x)$ for the exchange disordered spin $S = 1/2$ Heisenberg chain does not exhibit the characteristics expected for a fully many-body localized phase even at infinite disorder. Interestingly and in line with the observations made above, there are differences for spin length $S = 1$. While $s(x)$ also does not adopt the expected shape for a localized phase, it retains a peaked feature at the value of $\langle r \rangle \approx 0.5359$, along with a generally broadened background similar to the behavior of $S = 1/2$. This may be indicating that part of the system remains ergodic even in the infinite disorder limit $J/b \to 0$. These observations are in alignment with the notion that systems displaying nonabelian symmetries, as predicted by Vasseur *et al.*, do not enter a fully many-body localized phase. The distinctive nature of this incompletely many-body localized phase is also reflected in the failure of the probability distribution (Eq. (6)) to revert to the shape of the ergodic phase, as

one may expect in the absence of many-body localization. The origin of the differences between spin lengths $S = 1/2$ and $S = 1$ is less clear, but it could be related to the fundamentally different excitation spectra between integer and half-integer spin length isotropic Heisenberg chains of the type considered here [65–69]. Such a distinction, if relevant, is not anticipated for the anisotropic model Eq. (13), which would account for the absence of a similar dependence on S in the data of the local-field disordered chains in Fig. 3.

IV. SUMMARY AND OUTLOOK

Using methods developed in previous works [45], we studied the spectra of isotropic exchange-disordered spin chains (Eq. (1)) with respect to the probability distribution across samples. The latter reveals a transition from the ergodic phase at low to intermediate disorder strength to a phase qualitatively distinct from both the ergodic and the many-body localized phase. Such a phase has been theorized to result as a consequence of nonabelian symmetries, as present in Eq. (1), disrupting the formation of a sufficiently exhaustive set of local integrals of motion [70, 71] as required by many-body localization [36, 49]. The differences we find affect not just the averaged consecutive-gap ratio, but also the scaling behavior of the sample-to-sample standard deviation with system size and the probability distribution of the realization-specific average of the consecutive-gap ratio.

Moreover, our numerical data shows a qualitative difference between the spin lengths $S = 1/2$ and $S = 1$. This is in contrast to the local field disordered spin model (Eq. (13)) where no such qualitative difference between spin lengths has been observed [45]. Beyond the spectral information investigated here, future research may strive to use complimentary numerical methods [38, 63, 72] to verify the presence of this phase and elucidate its properties.

ACKNOWLEDGMENTS

We thank J. Richter for useful discussions and P. Wenk for technical help with the numerics. The work of J. Siegl was supported by Deutsche Forschungsgemeinschaft via SFB 1277. The data for the plots can be found at https://epub.uni-regensburg.de. Access to the code and to the raw numerical data is granted upon request to the corresponding author.

Appendix A: Occurrence of weak links

For disorder strengths $b \geq J$ the exchange parameters J_i can for some links approach zero. If at least two such "weak links" occur the connectivity of the system's Hilbert space changes as the chain effectively splits into two separate systems [37, 38]. This would impair the process of level repulsion whilst simultaneously realizing a trivial sense of localization distinct from the many-body localized phase. We briefly estimate the importance of the aforementioned mechanism for the presented results. We consider a data value to be affected by a weak link if at least two links in the corresponding realization are smaller than the average level spacing δ_i between multiplets in the respective S^z_{tot} subspace i from which the value was drawn. If we know the number of multiplets N_i in this subspace, the average level spacing can be upper bounded by

$$\delta_i \leq S^2(J + b)N/N_i. \tag{A1}$$

Given a specific δ, the probability for each individual link to be beneath this threshold is given by

$$q = \begin{cases} \Theta(b - J): & \delta \leq |J - b|, \\ (\delta - |J - b|)/2b: & |J - b| < \delta \leq J + b, \\ 1: & \delta > J + b. \end{cases} \tag{A2}$$

The probability of having at least two such links is

$$P_{\text{WL}} = 1 - (1 - q)^N - Nq(1 - q)^{N-1}, \tag{A3}$$

which for large N approaches

$$\lim_{N\to\infty} P_{\text{WL}} \approx 1 - e^{-c} - ce^{-c} \in [0, 1 - 2e^{-1}], \tag{A4}$$

where $c = \lim_{N\to\infty} Nq$. In the following we discuss $S = 1/2$, with similar findings holding for $S = 1$. For $i \geq N/2$ it holds

$$N_i = \binom{N}{i} - \binom{N}{i+1} = \frac{2i+1-N}{N+1}\binom{N+1}{i}. \tag{A5}$$

Therefore, the size of subspaces with low S^z_{tot} scales exponential in system size. This results in an exponential decrease of δ_i for these subspaces, which in turn guarantees $c = 0$ and $P_{\mathrm{WL}} \to 0$. Only the smallest subspace we consider, $S^z_{\mathrm{tot}} = S_{\mathrm{tot}} - 2$, has a finite c, as the number of multiplets within it scales only as N^2. In the process of evaluating $\langle r\rangle$ the probabilities are weighted by the number of multiplets in the respective subspace. Thus, the probability of any consecutive gap ratio to have been drawn from a disorder realization constituting a weak link still vanishes with increasing N. For the finite N considered in this work, the probability to encounter a weak link remains finite but small as shown in Fig. 5 (a).

The erroneous signal these few realizations would give when calculating $\langle r\rangle$ can be upper bounded by assuming that all data points that are not impacted by weak links follow GOE and all data points affected by weak links are fully Poissonian. This overestimates the false positive expected from the presence of weak links, but as shown in Fig. 5 (b), it does not match the transition observed in Fig. 2 either in magnitude, nor in its scaling behavior with system size.

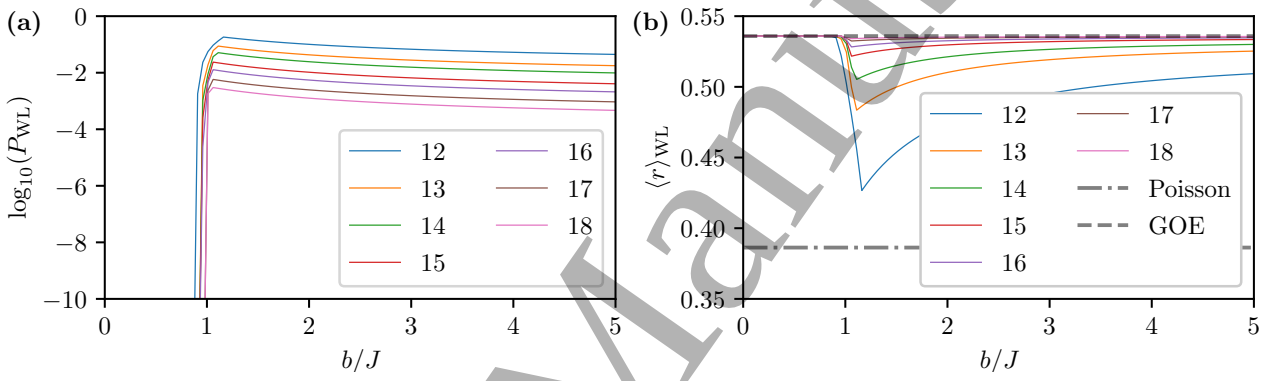

Figure 5. Probability of a multiplet being drawn from a realization affected by the presence of at least two weak links (a) and potential impact on the average consecutive gap ratio for $S = 1/2$ assuming all affected realizations yield a false signal equivalent to a fully localized phase (b). While the probability becomes finite close to $b \approx J$ as expected, we find it to remain small and consistently decreasing with system size N. The upper bound for the impact of the weak links is minimal already for the larger N we consider and is strongly decreasing with increasing system size, in line with the vanishing probabilities shown in (a). Neither the magnitude of the signal, nor its scalling with system size is compatible with the transition discussed in the main text. We thus exclude the fragmentation of the system's Hilbertspace due to weak links as the reason for the observed transition in $\langle r\rangle$.

[1] J. M. Deutsch, Quantum statistical mechanics in a closed system, Phys. Rev. A **43**, 2046 (1991).
[2] M. Srednicki, Chaos and quantum thermalization, Phys. Rev. E **50**, 888 (1994).
[3] M. Srednicki, The approach to thermal equilibrium in quantized chaotic systems, J. Phys. A: Math. Gen. **32**, 1163 (1999).
[4] R. Nandkishore and D. A. Huse, Many-Body Localization and Thermalization in Quantum Statistical Mechanics, Annu. Rev. Condens. Matter Phys. **6**, 15 (2015).
[5] L. D'Alessio, Y. Kafri, A. Polkovnikov, and M. Rigol, From quantum chaos and eigenstate thermalization to statistical mechanics and thermodynamics, Adv. Phys. **65**, 239 (2016).
[6] P. W. Anderson, Absence of Diffusion in Certain Random Lattices, Phys. Rev. **109**, 1492 (1958).
[7] N. F. Mott, M. Pepper, S. Pollitt, R. H. Wallis, and C. J. Adkins, The Anderson transition, Proc. R. Soc. Lond. A **345**, 169 (1975).
[8] C. J. Adkins, Threshold conduction in inversion layers, J. Phys. C: Solid State Phys. **11**, 851 (1978).
[9] D. A. Abanin, E. Altman, I. Bloch, and M. Serbyn, Colloquium: Many-body localization, thermalization, and entanglement, Rev. Mod. Phys. **91**, 021001 (2019).
[10] L. Fleishman and P. W. Anderson, Interactions and the Anderson transition, Phys. Rev. B **21**, 2366 (1980).
[11] A. M. Finkelstein, Influence of Coulomb interaction on the properties of disordered metals, JETP **57**, 97 (1983).
[12] T. Giamarchi and H. J. Schulz, Anderson localization and interactions in one-dimensional metals, Phys. Rev. B **37**, 325 (1988).

[13] B. L. Altshuler, Y. Gefen, A. Kamenev, and L. S. Levitov, Quasiparticle Lifetime in a Finite System: A Nonperturbative Approach, Phys. Rev. Lett. **78**, 2803 (1997).
[14] I. V. Gornyi, A. D. Mirlin, and D. G. Polyakov, Interacting Electrons in Disordered Wires: Anderson Localization and Low-T Transport, Phys. Rev. Lett. **95**, 206603 (2005).
[15] D. M. Basko, I. L. Aleiner, and B. L. Altshuler, Metal-insulator transition in a weakly interacting many-electron system with localized single-particle states, Ann. Phys. **321**, 1126 (2006).
[16] M. Schreiber, S. S. Hodgman, P. Bordia, H. P. Lüschen, M. H. Fischer, R. Vosk, E. Altman, U. Schneider, and I. Bloch, Observation of many-body localization of interacting fermions in a quasirandom optical lattice, Science **349**, 842 (2015).
[17] M. Žnidarič, T. Prosen, and P. Prelovšek, Many-body localization in the Heisenberg XXZ magnet in a random field, Phys. Rev. B **77**, 064426 (2008).
[18] V. Oganesyan, A. Pal, and D. A. Huse, Energy transport in disordered classical spin chains, Phys. Rev. B **80**, 115104 (2009).
[19] T. C. Berkelbach and D. R. Reichman, Conductivity of disordered quantum lattice models at infinite temperature: Many-body localization, Phys. Rev. B **81**, 224429 (2010).
[20] A. Pal and D. A. Huse, Many-body localization phase transition, Phys. Rev. B **82**, 174411 (2010).
[21] J. H. Bardarson, F. Pollmann, and J. E. Moore, Unbounded Growth of Entanglement in Models of Many-Body Localization, Phys. Rev. Lett. **109**, 017202 (2012).
[22] M. Serbyn, Z. Papić, and D. A. Abanin, Local Conservation Laws and the Structure of the Many-Body Localized States, Phys. Rev. Lett. **111**, 127201 (2013).
[23] M. Serbyn, Z. Papić, and D. A. Abanin, Criterion for Many-Body Localization-Delocalization Phase Transition, Phys. Rev. X **5**, 041047 (2015).
[24] T. E. O'Brien, D. A. Abanin, G. Vidal, and Z. Papić, Explicit construction of local conserved operators in disordered many-body systems, Phys. Rev. B **94**, 144208 (2016).
[25] V. Oganesyan and D. A. Huse, Localization of interacting fermions at high temperature, Phys. Rev. B **75**, 155111 (2007).
[26] D. J. Luitz, N. Laflorencie, and F. Alet, Many-body localization edge in the random-field Heisenberg chain, Phys. Rev. B **91**, 081103 (2015).
[27] T. Devakul and R. R. P. Singh, Early Breakdown of Area-Law Entanglement at the Many-Body Delocalization Transition, Phys. Rev. Lett. **115**, 187201 (2015).
[28] F. Pietracaprina, N. Macé, D. J. Luitz, and F. Alet, Shift-invert diagonalization of large many-body localizing spin chains, SciPost Phys. **5**, 045 (2018).
[29] E. V. H. Doggen, F. Schindler, K. S. Tikhonov, A. D. Mirlin, T. Neupert, D. G. Polyakov, and I. V. Gornyi, Many-body localization and delocalization in large quantum chains, Phys. Rev. B **98**, 174202 (2018).
[30] N. Macé, F. Alet, and N. Laflorencie, Multifractal Scalings Across the Many-Body Localization Transition, Phys. Rev. Lett. **123**, 180601 (2019).
[31] P. Sierant, M. Lewenstein, and J. Zakrzewski, Polynomially Filtered Exact Diagonalization Approach to Many-Body Localization, Phys. Rev. Lett. **125**, 156601 (2020).
[32] E. V. H. Doggen, I. V. Gornyi, A. D. Mirlin, and D. G. Polyakov, Many-body localization in large systems: Matrix-product-state approach, Ann. Phys. Special Issue on Localisation 2020, **435**, 168437 (2021).
[33] F. Evers and S. Bera, The internal clock of many-body (de-)localization (2023), arxiv:2302.11384 [cond-mat].
[34] D. Sels and A. Polkovnikov, Thermalization of Dilute Impurities in One-Dimensional Spin Chains, Phys. Rev. X **13**, 011041 (2023).
[35] J. Z. Imbrie, On Many-Body Localization for Quantum Spin Chains, J Stat Phys **163**, 998 (2016).
[36] A. C. Potter and R. Vasseur, Symmetry constraints on many-body localization, Phys. Rev. B **94**, 224206 (2016).
[37] I. V. Protopopov, W. W. Ho, and D. A. Abanin, Effect of SU(2) symmetry on many-body localization and thermalization, Phys. Rev. B **96**, 041122 (2017).
[38] I. V. Protopopov, R. K. Panda, T. Parolini, A. Scardicchio, E. Demler, and D. A. Abanin, Non-Abelian Symmetries and Disorder: A Broad Nonergodic Regime and Anomalous Thermalization, Phys. Rev. X **10**, 011025 (2020).
[39] The strong coupling case of one dimensional Hubbard chains at half filling is a spin 1/2-Heisenberg chain [73], implying a relation to the model studied in this work. For the disordered case and for the highly excited states relevant to MBL no mapping to the exchange disordered Heisenberg chain is known to the authors.
[40] P. Prelovšek, O. S. Barišić, and M. Žnidarič, Absence of full many-body localization in the disordered Hubbard chain, Phys. Rev. B **94**, 241104 (2016).
[41] M. Kozarzewski, P. Prelovšek, and M. Mierzejewski, Spin Subdiffusion in the Disordered Hubbard Chain, Phys. Rev. Lett. **120**, 246602 (2018).
[42] S. J. Thomson, Disorder-induced spin-charge separation in the one-dimensional Hubbard model, Phys. Rev. B **107**, L180201 (2023).
[43] C. Murthy, A. Babakhani, F. Iniguez, M. Srednicki, and N. Yunger Halpern, Non-Abelian Eigenstate Thermalization Hypothesis, Phys. Rev. Lett. **130**, 140402 (2023).
[44] S. Majidy, A. Lasek, D. A. Huse, and N. Y. Halpern, Non-Abelian symmetry can increase entanglement entropy, Phys. Rev. B **107**, 045102 (2023), arxiv:2209.14303 [cond-mat, physics:hep-th, physics:quant-ph].
[45] J. Schliemann, J. V. I. Costa, P. Wenk, and J. C. Egues, Many-body localization: Transitions in spin models, Phys. Rev. B **103**, 174203 (2021).
[46] This corresponds to the model used in Ref. [38] for their parameters $\alpha = 1.0$, but with varying μ.
[47] R. Vasseur, A. C. Potter, and S. A. Parameswaran, Quantum Criticality of Hot Random Spin Chains, Phys. Rev. Lett.

114, 217201 (2015).
[48] Y. Y. Atas, E. Bogomolny, O. Giraud, and G. Roux, Distribution of the Ratio of Consecutive Level Spacings in Random Matrix Ensembles, Phys. Rev. Lett. **110**, 084101 (2013).
[49] D. A. Abanin and Z. Papić, Recent progress in many-body localization, Ann. Phys. **529**, 1700169 (2017).
[50] E. Altman and R. Vosk, Universal Dynamics and Renormalization in Many-Body-Localized Systems, Annu. Rev. Condens. Matter Phys. **6**, 383 (2015).
[51] J. Z. Imbrie, V. Ros, and A. Scardicchio, Local integrals of motion in many-body localized systems, Ann. Phys. **529**, 1600278 (2017).
[52] K. Agarwal, E. Altman, E. Demler, S. Gopalakrishnan, D. A. Huse, and M. Knap, Rare-region effects and dynamics near the many-body localization transition, Ann. Phys. **529**, 1600326 (2017).
[53] D. J. Luitz and Y. B. Lev, The ergodic side of the many-body localization transition, Ann. Phys. **529**, 1600350 (2017).
[54] A. Haldar and A. Das, Dynamical many-body localization and delocalization in periodically driven closed quantum systems, Ann. Phys. **529**, 1600333 (2017).
[55] J. Gu, S. Liu, M. Yazback, H.-P. Cheng, and X.-G. Zhang, Many-body localization from random magnetic anisotropy, Phys. Rev. Res. **1**, 033183 (2019).
[56] J. Richter, D. Schubert, and R. Steinigeweg, Decay of spin-spin correlations in disordered quantum and classical spin chains, Phys. Rev. Res. **2**, 013130 (2020).
[57] T. Chanda, P. Sierant, and J. Zakrzewski, Time dynamics with matrix product states: Many-body localization transition of large systems revisited, Phys. Rev. B **101**, 035148 (2020).
[58] M. Kiefer-Emmanouilidis, R. Unanyan, M. Fleischhauer, and J. Sirker, Slow delocalization of particles in many-body localized phases, Phys. Rev. B **103**, 024203 (2021).
[59] A. Morningstar, L. Colmenarez, V. Khemani, D. J. Luitz, and D. A. Huse, Avalanches and many-body resonances in many-body localized systems, Phys. Rev. B **105**, 174205 (2022).
[60] D. Sels, Bath-induced delocalization in interacting disordered spin chains, Phys. Rev. B **106**, L020202 (2022).
[61] P. Sierant and J. Zakrzewski, Challenges to observation of many-body localization, Phys. Rev. B **105**, 224203 (2022).
[62] We refer to the limit $J/b \to 0$ as infinite disorder. This is distinct from the notion adopted in Ref. [38], where the authors varied the shape of the distribution for fixed $J = 0$.
[63] D. Saraidaris, J.-W. Li, A. Weichselbaum, J. von Delft, and D. A. Abanin, Finite-size subthermal regime in disordered SU(N)-symmetric Heisenberg chains (2023), arxiv:2304.03099 [cond-mat, physics:quant-ph].
[64] See Fig. 6 of Ref. [38] for $\alpha = 1.0$.
[65] F. D. M. Haldane, Continuum dynamics of the 1-D Heisenberg antiferromagnet: Identification with the O(3) nonlinear sigma model, Physics Letters A **93**, 464 (1983).
[66] F. D. M. Haldane, Nonlinear Field Theory of Large-Spin Heisenberg Antiferromagnets: Semiclassically Quantized Solitons of the One-Dimensional Easy-Axis N\'eel State, Phys. Rev. Lett. **50**, 1153 (1983).
[67] F. D. M. Haldane, "Θ physics" and quantum spin chains (abstract), Journal of Applied Physics **57**, 3359 (1985).
[68] I. Affleck, Quantum spin chains and the Haldane gap, J. Phys.: Condens. Matter **1**, 3047 (1989).
[69] T. Jolicoeur and O. Golinelli, Physics of integer-spin antiferromagnetic chains: Haldane gaps and edge states, Comptes Rendus Chimie **22**, 445 (2019).
[70] A. Chandran, I. H. Kim, G. Vidal, and D. A. Abanin, Constructing local integrals of motion in the many-body localized phase, Phys. Rev. B **91**, 085425 (2015).
[71] S. J. Thomson and M. Schiró, Time evolution of many-body localized systems with the flow equation approach, Phys. Rev. B **97**, 060201 (2018).
[72] T. Macrì, L. Lepori, G. Pagano, M. Lewenstein, and L. Barbiero, Bound state dynamics in the long-range spin-$\frac{1}{2}$ XXZ model, Phys. Rev. B **104**, 214309 (2021).
[73] F. H. L. Essler, H. Frahm, F. Göhmann, A. Klümper, and V. E. Korepin, *The One-Dimensional Hubbard Model* (Cambridge University Press, Cambridge, 2005).